Journal of Photonics for Energy

PhotonicsforEnergy.SPIEDigitalLibrary.org

Annihilation upconversion: harvesting the entire deep-red spectral range of the sun irradiation

Ernesta Heinrich
Yuri Avlasevich
Katharina Landfester
Stanislav Baluschev

SPIE.

Ernesta Heinrich, Yuri Avlasevich, Katharina Landfester, Stanislav Baluschev, "Annihilation upconversion: harvesting the entire deep-red spectral range of the sun irradiation," *J. Photon. Energy* **8**(2), 022002 (2017), doi: 10.1117/1.JPE.8.022002.

Annihilation upconversion: harvesting the entire deep-red spectral range of the sun irradiation

Ernesta Heinrich,[a] Yuri Avlasevich,[a] Katharina Landfester,[a] and Stanislav Baluschev[a,b,*]

[a]Max Planck Institute for Polymer Research, Department of Physical Chemistry of Polymers, Mainz, Germany

[b]Sofia University "St. Kliment Ochridski," Department of Optics and Spectroscopy, Sofia, Bulgaria

Abstract. Solar energy storage and conversion is a key technology for the future realization of a sustainable energy production worldwide. The utilization of low-energy photons by means of upconversion (UC) processes has the main advantage of the upconversion process and solar energy-harvesting devices being considered and optimized independently, without affecting the particular physical characteristics of the operating sunlight excited material or device architectures. The UC-device must function efficiently with noncoherent light excitation, under light intensities comparable with those obtainable from moderate concentrated sunlight (1 to 20 suns, AM1.5); such a low degree of concentration allows usage of Fresnel-type focusing systems. We report chemical synthesis and efficient functioning of a triplet–triplet annihilation upconversion-based device, harvesting the entire deep-red spectral range of the sun irradiation ($\Delta\lambda \sim 142$ nm) in a gap-free manner. © *2017 Society of Photo-Optical Instrumentation Engineers (SPIE)* [DOI: 10.1117/1.JPE.8.022002]

Keywords: sunlight; deep-red region; photon upconversion; triplet–triplet annihilation; metallated macrocycles.

Paper 17089SS received Aug. 29, 2017; accepted for publication Sep. 26, 2017; published online Nov. 6, 2017.

1 Introduction

Solar energy storage and conversion is a key technology for the future realization of sustainable energy production worldwide. The utilization of low-energy photons by means of upconversion processes contrasts with the other sunlight harvesting concepts, which all focus on the development of the solar devices themselves to match better the polychromatic solar spectrum. This is usually done either by widening their absorption spectrum or by building multijunction devices.[1,2] The main advantage of the photon upconversion technique is that the upconversion process and solar energy-harvesting devices can be considered and optimized independently, without affecting the particular physical characteristics of the operating sunlight excited material or device architectures. As an outcome, a well-developed photon upconversion device (UCd) can be combined with different existing solar energy-harvesting devices.

The specific application of photon upconversion in solar energy-harvesting devices is only possible when the following requirements are fulfilled: to start, the UCd must function efficiently with noncoherent light excitation; further, the excitation intensity necessary for effective UC needs to be small (as low as 1 $\mathrm{Wcm^{-2}}$)—comparable with light intensities obtainable from moderate concentrated sunlight (1 to 20 suns, AM1.5), such a degree of concentration is obtainable by nominating Fresnel-type optical systems; and last, the excitation spectral power density required for effective UCd needs to be comparable with those of the terrestrial sun irradiation (in order of 100 $\mu\mathrm{Wnm^{-1}}$).

*Address all correspondence to: Stanislav Baluschev, E-mail: balouche@mpip-mainz.mpg.de

1947-7988/2017/$25.00 © 2017 SPIE

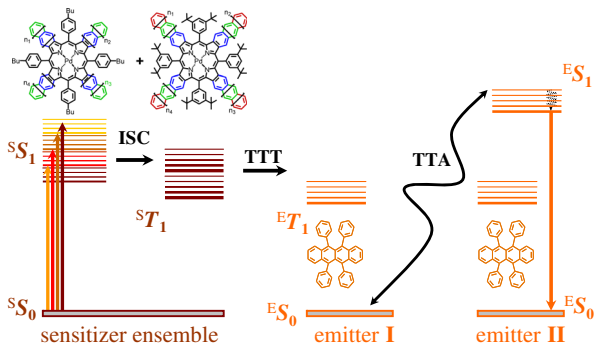

Fig. 1 Simplified energetic scheme of the TTA-UC process in multicomponent organic system. Upper—general structures of the sensitizer ensemble, right—structure of the emitter (rubrene).

Triplet–triplet annihilation upconversion (TTA-UC) is the only upconversion method that has been experimentally demonstrated to operate with noncoherent low-intensity illumination, such as moderate concentrated sunlight.[3,4] Such a low-energy threshold allows for the development of several unique applications in material science,[5–7] solar cell devices,[8,9] solar fuels,[10] bioimaging,[11,12] and extension of the infrared limit of oxygenic photosynthesis.[13,14] The TTA-UC process takes place in multichromophore systems consisting of energetically optimized pairs of sensitizer (transition metal chelates and macrocycles) and emitter molecules (polycyclic aromatic hydrocarbons or BODIPYs); shortly, photon energy absorbed by the Q-band of a sensitizer (Fig. 1) is stored in its triplet state, formed via the process of intersystem crossing. Further, this energy is transferred to an emitter triplet state in a process of triplet–triplet energy transfer. Next, the excited triplet states of two emitter molecules undergo TTA, in which one emitter molecule returns back to its singlet ground state and the other molecule gains the energy of both triplet states and is excited to a higher energy singlet state. As the singlet state emitter decays radiatively back to the ground state, a fluorescence photon is emitted, which is strongly blueshifted compared with the excitation photons.

The quantum yield ($QY_{TTA\text{-}UC}$) of the TTA-UC process is certainly of decisive importance for when further applications in solar energy-harvesting devices are planned. It has to be pointed out that a classical term (such as quantum yield) is attributed to a complex system, such as the TTA-UC process. In our study, we use the term quantum yield in a classical meaning: the "absorption" of the UC-media will be determined by the Q-band absorption of the used sensitizer, and the "emission" will be attributed to the UC-fluorescence of the emitter species: $QY_{TTA\text{-}UC} = N^{photons}_{emitted}/N^{photons}_{absorbed}$. In a soft matter matrix, the TTA process is diffusion controlled, demonstrating essential dependences on the material and environmental parameters, such as the degree of overlapping of the interacting energy states, matrix temperature, matrix viscosity, and presence of molecular oxygen. In the presence of molecular oxygen, the energy stored in the excited states of the triplet ensembles is being actively dissipated, competing with emissive (phosphorescence) or nonemissive (triplet to triplet) energy transfer processes. The reason for this is the process energy transfer between the organic molecule triplet state and the ground state of molecular oxygen leads to the generation of singlet oxygen.[15] Singlet oxygen is a highly reactive species causing oxidation of the photoactive molecules, followed by further loss of efficiency. In fact, even very small oxygen concentrations on the level of 2 to 10 ppm could affect the TTA-UC efficiency substantially.[16] Therefore, to fully exploit the TTA-UC process in different applications, the development of an effective protection strategy against quenching by molecular oxygen and against the subsequent production of highly reactive singlet oxygen is essential.[17,18]

2 Methodology

2.1 *General Remarks*

The solvents and reagents were either prepared in the laboratory according to the described procedure or purchased commercially from Sigma–Aldrich, Acros, or Roth and used as obtained. Cyclohexanon 1, naphthalene 5, and 1,2-dibromobenzene 14 were commercially

obtained. Deuterated solvents used for ^{1}H-NMR spectroscopy were bought from Deutero GmbH. Dry dichloromethane (DCM) was acquired by distillation of a CaH_2 mix. The silica powder necessary for preparative column chromatography with the particle size of 0.063 to 0.200 mm was purchased from Marchery–Nagel. ^{1}H-NMR spectra were recorded at 250 MHz with a liquid-state spectrometer Bruker DPX 250. The mass of the compounds was obtained via conducted field desorption mass spectrometry with a ZAB 2-SE-FPD instrument by VG Analytical. Absorption spectra were acquired via a PerkinElmer Lambda 25 UV/Vis spectrometer.

The synthesis of mixed porphyrins is based on assembly of "benzo-" (Fig. 2), "naphtho-" (Fig. 3) and "anthra-" building blocks (Fig. 4). The general reaction scheme follows a modified version of the porphyrin synthesis first reported by Finikova et al.[19] and Brunel et al.[20] Cyclohexene (or its derivative) is transformed into a cyclic alpha vinyl sulfone[21,22] and further reacts with tert-butylisocyanate to form tert-butyl-4,5,6,7-tetrahydro-2H-isoindole-1-carboxylate. Boiling in the presence of potassium hydroxide yields 4,5,6,7-tetrahydro-2H-isoindole. The isolation of the individual porphyrins with a fixed number of benzo and naphtho moieties from the mixture can be achieved by two routes. First is the isolation of free-base porphyrins by chromatography and the metal insertion into the individual substances. Second is the metal insertion into the porphyrins mixture and subsequent separation of the metalloporphyrins. Using the first route, only a negligible amount of the target compounds could be isolated after several subsequent chromatographic separations. The second approach shows that the Pd-porphyrins move on the TLC plate and on the column as a single zone and cannot be separated. However, the mixture of Pd-porphyrins could be isolated in a high yield, showing a sharp Soret band and Q-bands forming a broad absorption band between 620 and 790 nm.

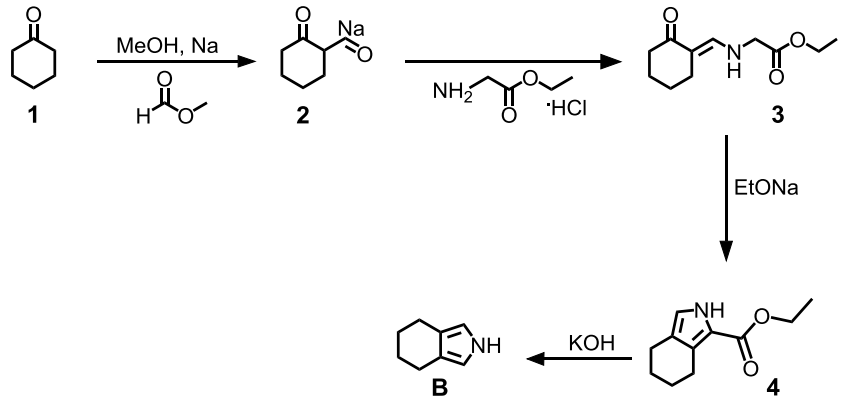

Fig. 2 Synthetic procedure for the benzo-building block starting from cyclohexanone **1**.

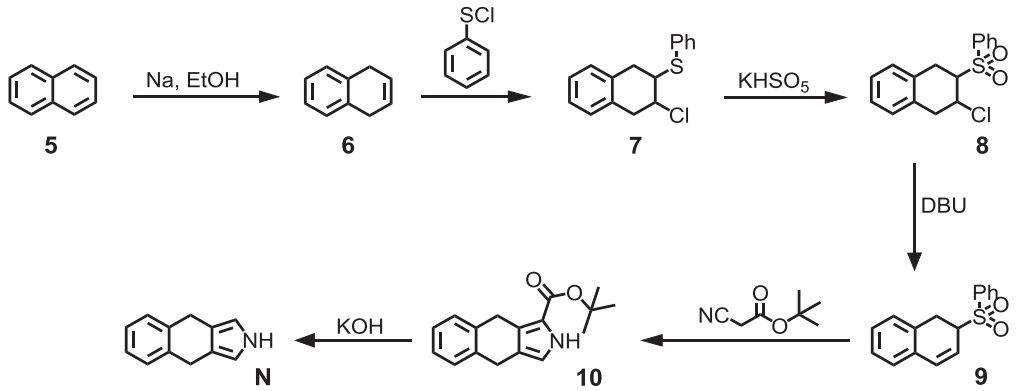

Fig. 3 Synthetic procedure for the naphtho-building block starting from naphthalene **5**.

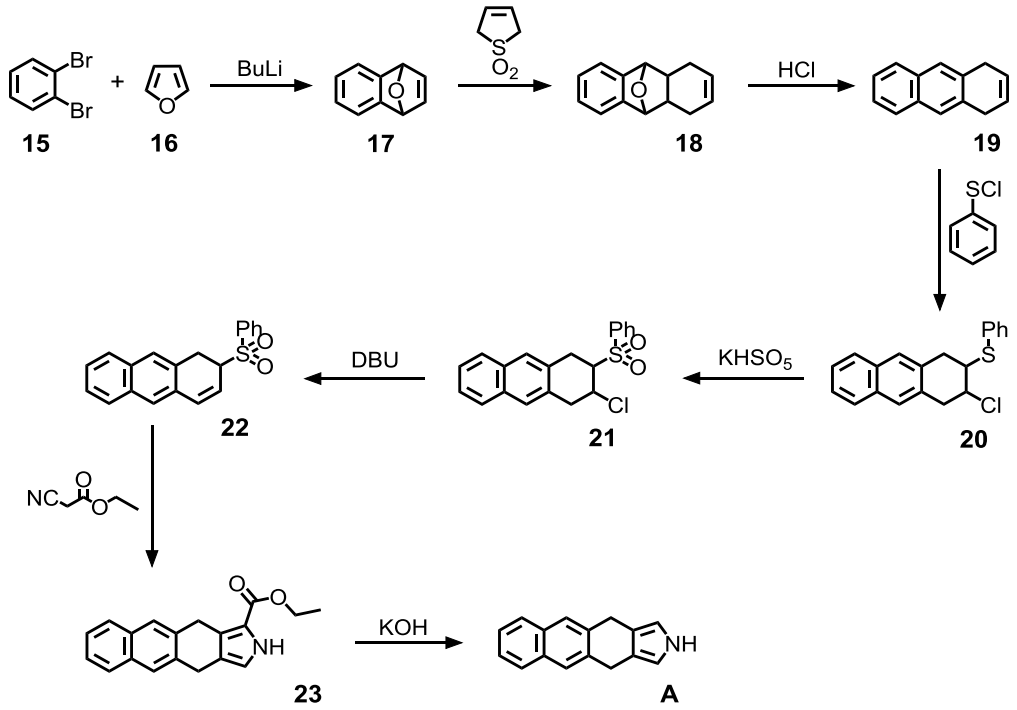

Fig. 4 Synthetic procedure for the anthra-building block starting from 1,2-dibromobenzene **15**.

2.2 *Mixed Benzo-Naphtho Porphyrin Family (12)*

A mixture of 4,5,6,7-tetrahydro-2H-isoindole **B** (0.143 g, 1.18 mmol), 4,9-dihydro-2H-benzo[*f*] isoindole **N** (0.200 g, 1.18 mmol), and 4-butylbenzaldehyde **11** (0.383 g, 2.36 mmol) in 200 mL of CH_2Cl_2, which was freshly distilled from CaH_2, was stirred for 10 min at room temperature under nitrogen. After addition of the catalyst $BF_3 \cdot Et_2O$ (0.033 g, 0.236 mmol), the mixture was stirred for 1 h. Following the addition of DDQ (0.268 g, 1.18 mmol), it was stirred once again for 1 h. Afterward, the mixture was washed with aqueous Na_2SO_3 and dried over Na_2SO_4, and the solvent was evaporated in vacuum. The crude product was purified on a silica gel column (eluent CH_2Cl_2) resulting in 0.755 g of the mixed benzo-naphtho porphyrin family **12** (Fig. 5).

2.3 *Metallated Mixed Benzo-Naphtho Porphyrin Family (13)*

The mixture of porphyrin **12** (0.500 g), bis(benzonitrile)palladium(II)chloride (0.120 g, 0.31 mmol), and trimethylamine (0.222 g, 2.50 mmol) in benzonitrile (30 mL) was refluxed for 1 h under nitrogen atmosphere. After complete metal insertion, the reaction mixture was allowed to cool down to room temperature. The solvent was evaporated in vacuum. The remaining Pd black was separated from the crude product via dissolving in CH_2Cl_2 and filtering through a thin layer of celite. Purification was carried out by chromatography on silica gel using CH_2Cl_2 as an eluent yielding 0.398 g of mixed benzo-naphtho porphyrin family **13**.

2.4 *Aromatized Mixed Benzo-Naphtho Porphyrin Family (14)*

A mixture of the mixed porphyrin family **13** (0.200 g) and DDQ (0.215 g, 0.94 mmol) in THF was refluxed for 20 to 40 min. After complete aromatization, the mixture was allowed to cool down to room temperature. The volume of the solvent was increased, and the mixture was washed with a 10% aqueous solution of Na_2SO_3, followed by brine, and dried over Na_2SO_4. The solvent was evaporated in vacuum, and the crude product was purified on a silica gel column (eluent: CH_2Cl_2) yielding 0.160 g of the mixed benzo-naphtho porphyrin family **14**. The FD-Mass (HABA matrix) is m/z: 1565.3, 1618.6, 1669.2, 1717.7, and 1770.8; the calculated is 1568.50, 1618.56, 1668.62, 1718.68, and 1768.74, respectively.

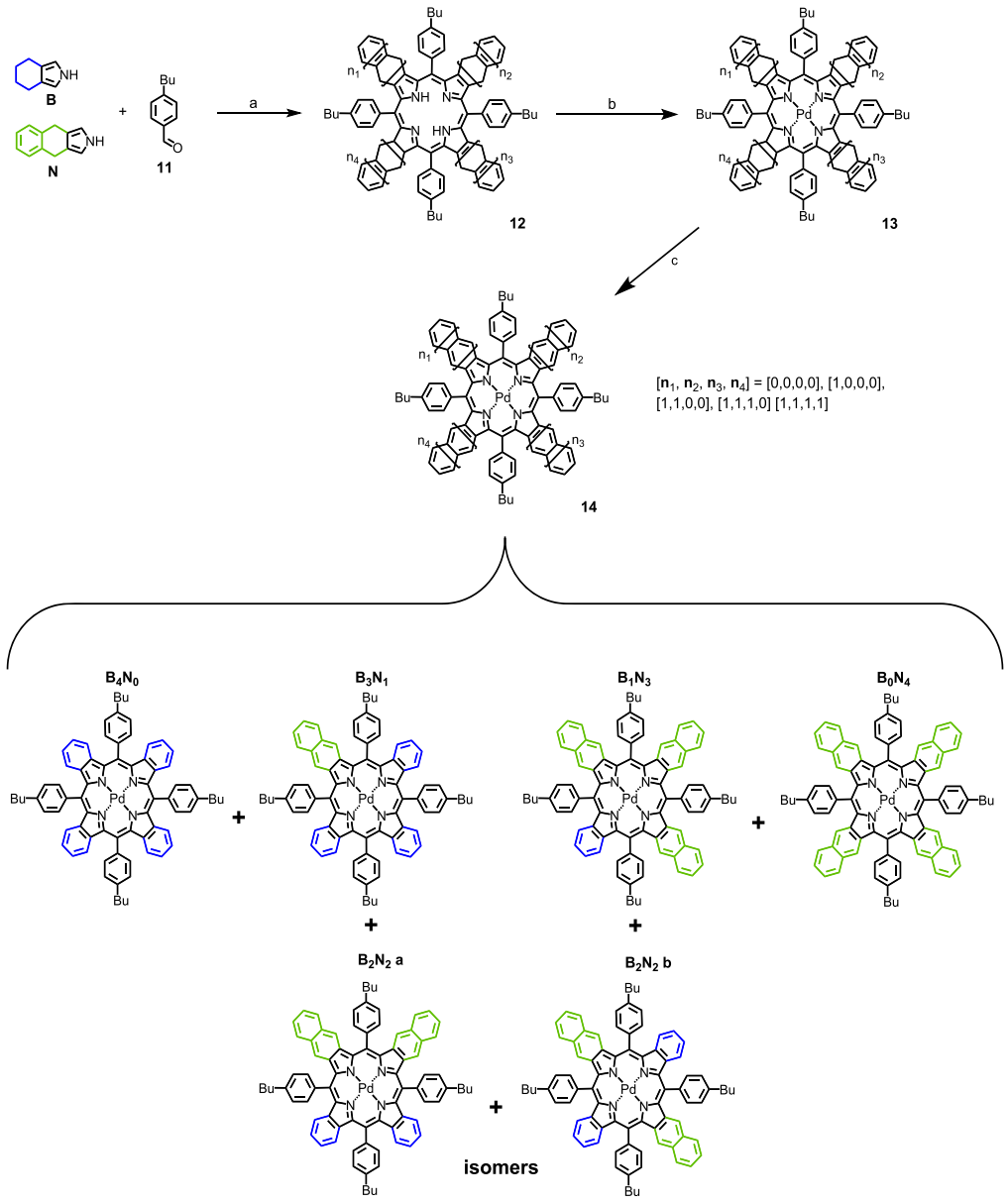

Fig. 5 Synthetic route for obtaining the mixed benzo-naphtho porphyrin family. Reaction conditions as follows: (a) (i) CH_2Cl_2, $BF_3 \cdot Et_2O$, 1 h, 20°C; (i) 2,3-Dichloro-5,6-dicyano-1,4-benzoquinone (DDQ), 1 h, 20°C; (b) bis(benzonitrile)palla-dium(II)chloride, NEt_3, benzonitrile, reflux, 1 h; and (c) DDQ, tetrahydrofurane (THF), reflux, 20 to 40 min.

2.5 *Mixed Naphtho-Anthra Porphyrin Family (25)*

A mixture of 4,9-dihydro-2*H*-benzo[*f*]isoindole N (0.210 g, 1.24 mmol), 4,11-dihydro-2H-naphtho[2,3-*f*]isoindole A (0.271 g, 1.24 mmol), and 3,5-di-tert-butylbenzaldehyde **24** (0.541 g, 2.48 mmol) in 250 mL of CH_2Cl_2, which was freshly distilled from CaH_2, was stirred for 10 min at room temperature under nitrogen. After addition of the catalyst $BF_3 \cdot Et_2O$ (0.035 g, 0.248 mmol), the mixture was stirred for 1 h. Following the addition of DDQ (0.422 g, 1.86 mmol), it was stirred once again for 1 h. Afterward, the mixture was washed with aqueous Na_2SO_3 and dried over Na_2SO_4, and the solvent was evaporated in vacuum. The crude product was purified on a silica gel column (eluent CH_2Cl_2) resulting in 0.245 g of the mixed naphtho-anthra porphyrin family **25** (Fig. 6).

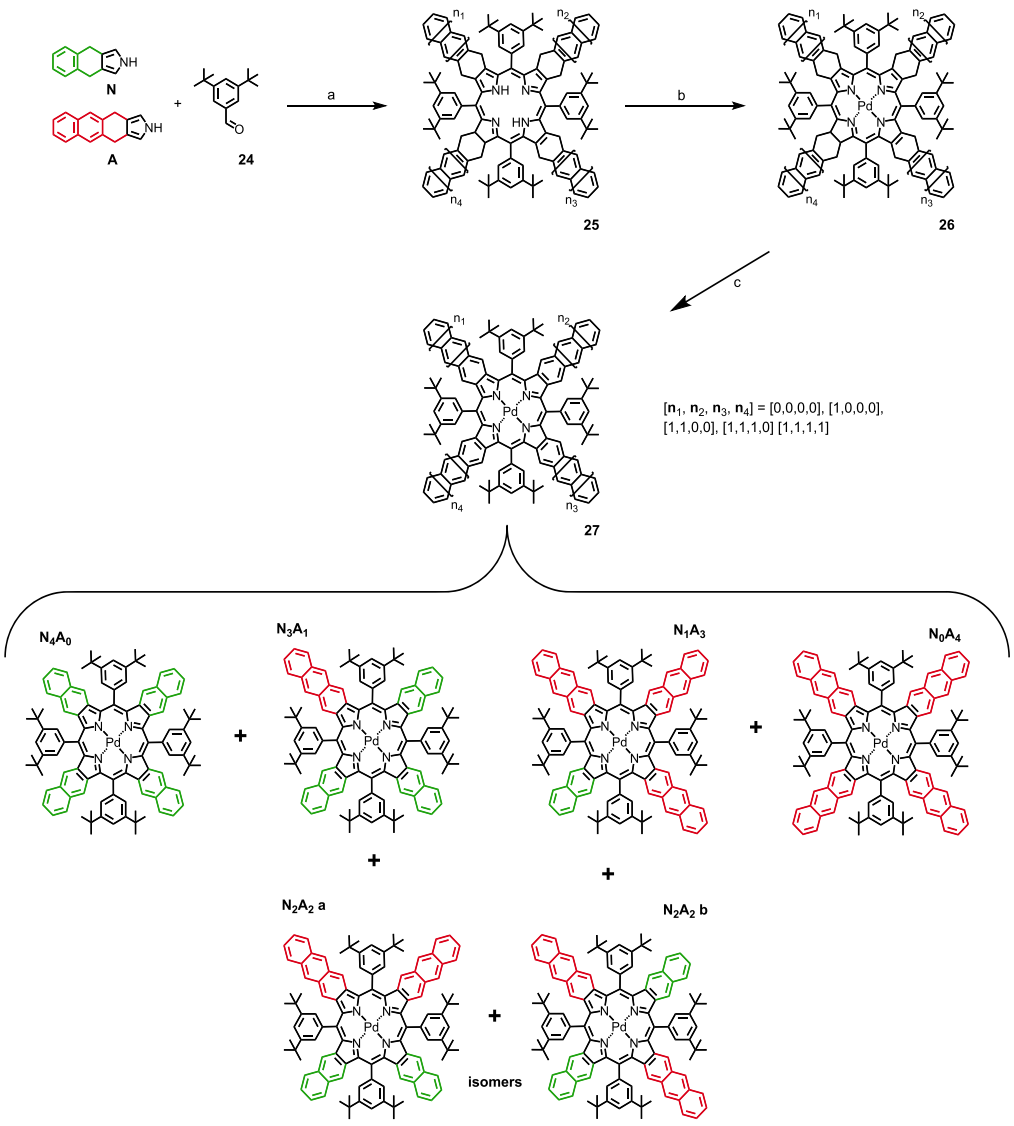

Fig. 6 Synthetic route for obtaining the mixed naphtho-anthra porphyrin family. Reaction conditions as follows: (a) (i) CH_2Cl_2, $BF_3 \cdot Et_2O$, 1 h, 20°C; (i) DDQ, 1 h, 20°C; (b) bis(benzonitrile)palladium(II)chloride, NEt_3, benzonitrile, reflux, 1 h; and (c) DDQ, THF, reflux, 20 to 40 min.

2.6 *Metallated Mixed Naphtho-Anthra Porphyrin Family (26)*

The mixture of porphyrin **25** (0.2 g), bis(benzonitrile)palladium(II)chloride (0.078 g, 0.204 mmol), and trimethylamine (0.101 g, 1 mmol) in benzonitrile (10 mL) was refluxed for 1 h under nitrogen atmosphere. After complete metal-insertion, the reaction mixture was allowed to cool down to room temperature. The solvent was evaporated in vacuum. The remaining Pd black was separated from the crude product via dissolving in CH_2Cl_2 and filtrating through a thin layer of celite. Purification was carried out by chromatography on silica gel using CH_2Cl_2 as an eluent yielding 0.221 g of mixed naphtho-anthra porphyrin family **26**.

2.7 *Aromatized Mixed Naphtho-Anthra Porphyrin Family (27)*

A mixture of the mixed porphyrin family **26** (0.1 g) and DDQ (0.187 g, 0.82 mmol) in THF was refluxed for 20 to 40 min. After complete aromatization, the mixture was allowed to cool down to room temperature. The volume of the solvent was increased, and the mixture was washed with a 10% aqueous solution of Na_2SO_3, followed by brine, and dried over Na_2SO_4. The solvent was

evaporated in vacuum, and the crude product was purified on a silica gel column (eluent: CH_2Cl_2) yielding 0.94 g of the mixed naphtho-anthra porphyrin family **27**. The FD-Mass (HABA matrix) is m/z: 1565.3 (39), 1618.6 (65), 1669.2 (100), 1717.7 (44), and 1770.8 (20); the calculated is 1568.50, 1618.56, 1668.62, 1718.68, and 1768.74, respectively.

3 Results

Figures 7(a) and 7(b) show the absorption spectra of the synthesized sensitizer families—the mixed benzo-naphtho porphyrin family (**14**) and mixed naphtho-anthra porphyrin family (**27**), respectively.

For characterization of the TTA-UC systems, an experimental setup emulating sunlight excitation with low degree of concentration was used. The supercontinuum laser source

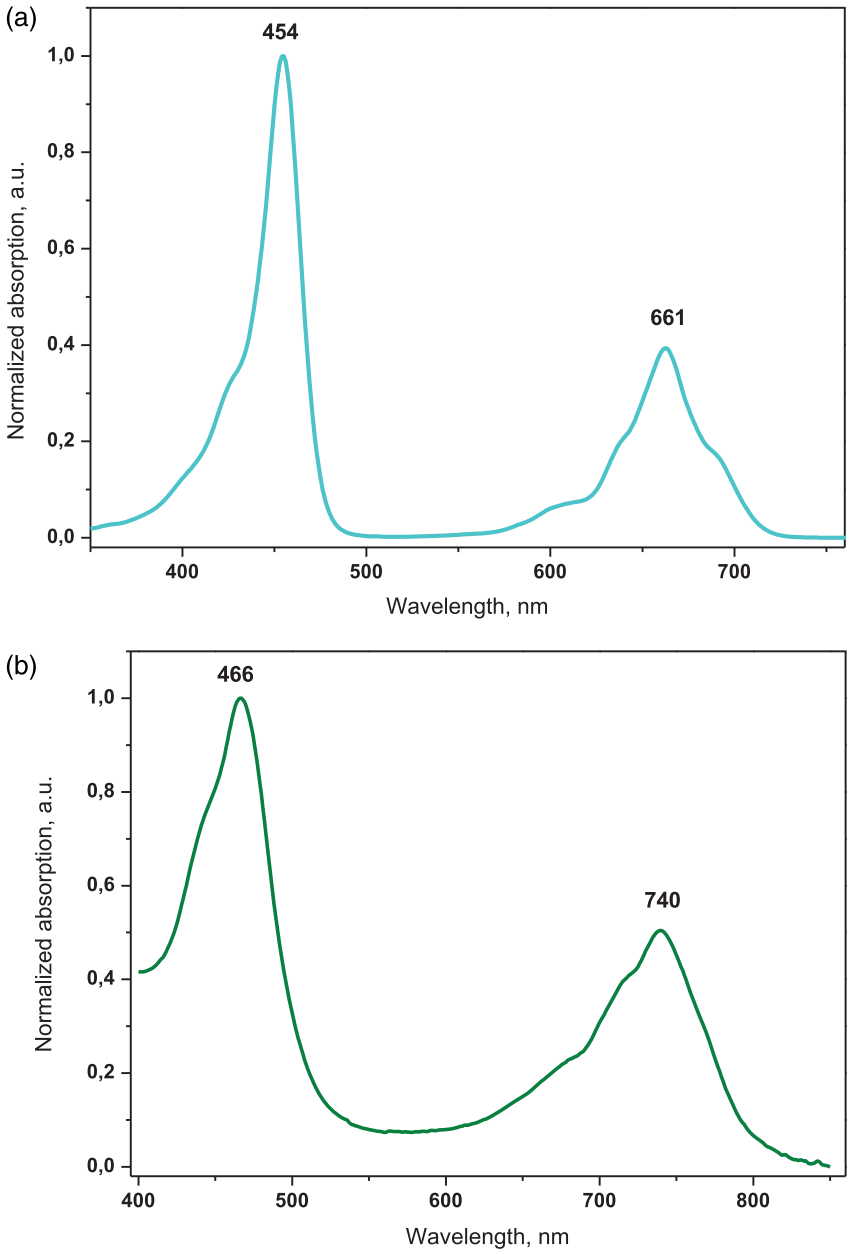

Fig. 7 Normalized absorption spectra of (a) mixed benzo-naphtho porphyrin family (**14**) and (b) mixed naphtho-anthra porphyrin family (**27**), both measured in toluene.

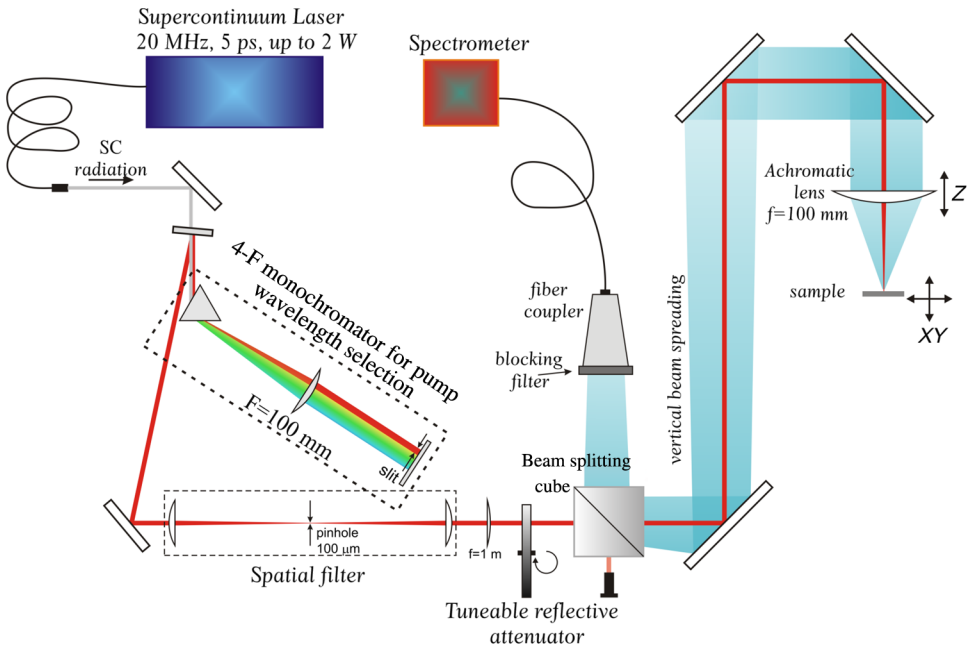

Fig. 8 Experimental setup for measurement of the TTA-UC quantum yield. To minimize the effect of solvent convection, the liquid samples are measured in the horizontal position.

(SC400-2-PP, Fianium Ltd.) delivers quasimonochromatic light with a mean power up to 2 W and 20 MHz repetition rate (Fig. 8) at an intensity comparable with 1/100 Suns (AM1.5). This light source can produce an excitation spectrum with a freely chosen bandwidth. Thus, the Q-band absorption spectrum of each sensitizer can be covered completely [Fig. 9(a)]. This is achieved via a 4-F monochromator and a retroreflector equipped with mechanical optical slit for precise selection of the excitation wavelength. The spatial distribution of the excitation beam is Gaussian, TEM_{00} mode, and beam waist ~1300 μm. The beam waist is controlled by Slit Scanning Beam Profiler (BP104-VIS, Thorlabs Inc.). The emission spectra were registered by Optical Multichannel Analyzer (Hamamatsu Inc.).

The excitation laser wavelengths were effectively suppressed (more than 10^5 times) using a custom-made super broad notch filter (ZET690/140nf, AHF Analyzenthechnik GmbH); in Fig. 9(b), the filter transmission is shown. In a standard procedure, the solutions of UC active compounds are filled into an optical glass tube prepared and sealed in a nitrogen-filled glove box using dry organic solvents.

In Fig. 10, the absorption spectrum of a sensitizer ensemble composed from a benzo-naphtho porphyrin family (**14**) and naphtho-anthra porphyrin family (**27**) is shown. The Q-band absorption covers the entire deep-red region of the terrestrial sun irradiation. The spectral width of the excitation spectrum (defined at FWHM) is more than $\Delta\lambda \sim 142$ nm. This allows harvesting the complete sunlight energy of the deep-red region and transferring it via the TTA-UC in visible light, accessible for further use through any type of energy storage technology.

The fluorescence spectrum of the emitter molecule (rubrene) working effectively with every single sensitizer from the benzo-naphtho porphyrin family (**14**) and naphtho-anthra porphyrin family (**27**) is shown in Fig. 10. It is important to notice that emitter fluorescence spectrum matches well with the transparency window of the sensitizer ensemble; thus, no parasitic reabsorption of the generated UC-emission was observed. The extremely broad excitation spectrum of the sensitizer ensemble combined with the energetically well-situated transparency window explains the observed high overall TTA-UC quantum yield—on the level of 0.04 (following the classical definition) measured at total excitation intensity of 100 $mWcm^{-2}$, obtained by a superbroad excitation spectrum as shown in Fig. 9(a). At sunlight concentration of 11 times (AM1.5), the observed TTA-UC yield was 0.038. The UC-samples were prepared and sealed in a nitrogen-filled glove box at an oxygen level <2 ppm; the solvent was dry hexadecane. The emitter concentration was 2×10^{-4} M, and the total sensitizer concentration was $\sim 1 \times 10^{-5}$ M.

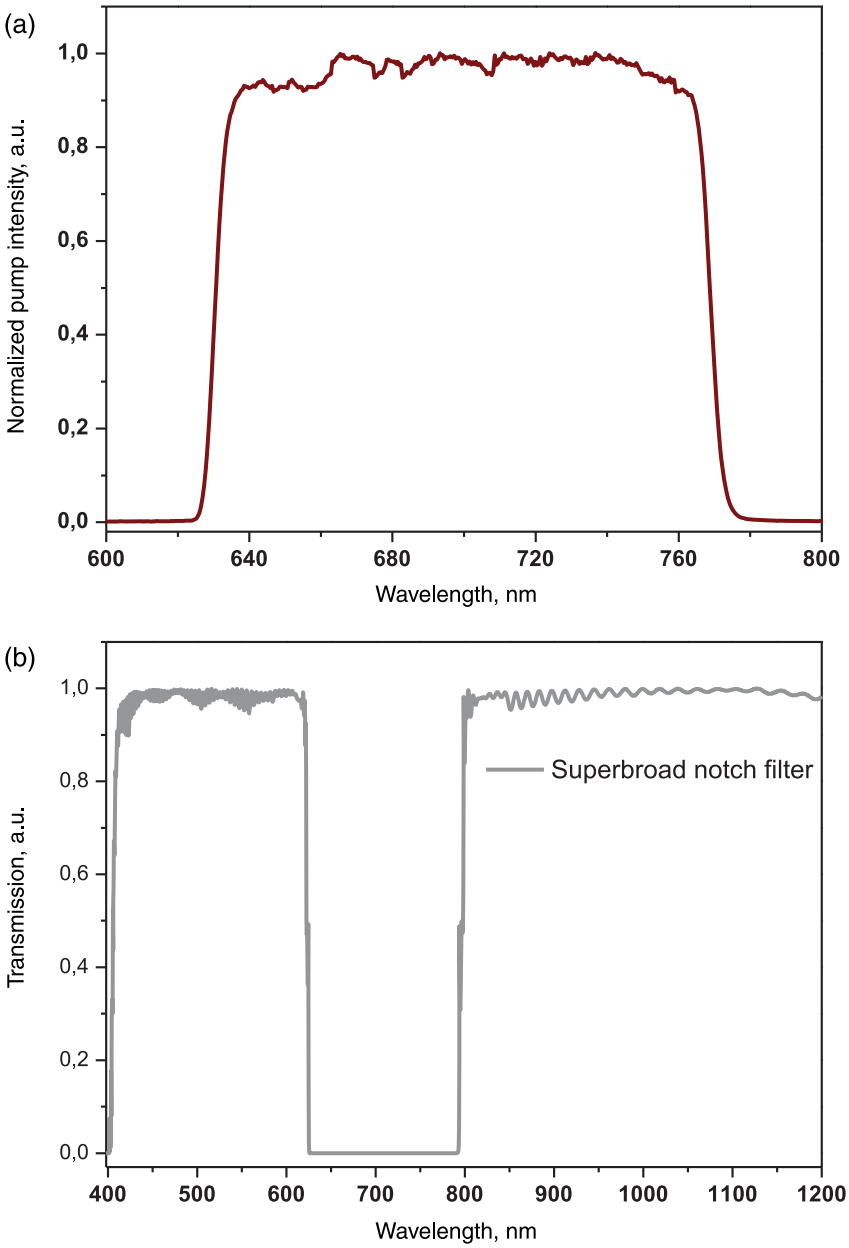

Fig. 9 (a) Excitation spectrum and (b) transmission spectrum of the broadband notch filter.

Under very low-excitation intensity of 1 Sun (AM1.5, the total light intensity harvested by the integral Q-band of the sensitizer ensemble is estimated to be 9.5 $\mathrm{mWcm^{-2}}$), the overall UC quantum yield is significantly lower—on the level of 0.017. For a broad range of excitation intensities (from 0.2 Sun up to 20 Sun), the dependence of the TTA-UC quantum yield for the studied system can be interpolated with a function $Q.Y._{\mathrm{UC}} \sim I_{\mathrm{EXC}}^{b}$, where $b = 1.3$.

This extremely broad excitation spectrum solves another technological problem, limiting the sunlight-based energy storage technologies: UC-devices application should require as low as possible sunlight concentration and allow application of nonimaging optical devices, such as solar concentrators based on Fresnel lenses[23] or 2-D polymer microlens arrays. Even a very low sunlight concentration ratio (<10 times) obtained by Fresnel–Köhler flat optical design[24] lenses, aspheric lenses created on a flat polymer substrate,[25] polymer microlens arrays obtained by ink-jet printing technique,[26] or microlens arrays based on polymer network liquid crystal[27,28] allows the effective transformation of the deep-red sunlight spectral range via the studied process of TTA-UC in visible light.

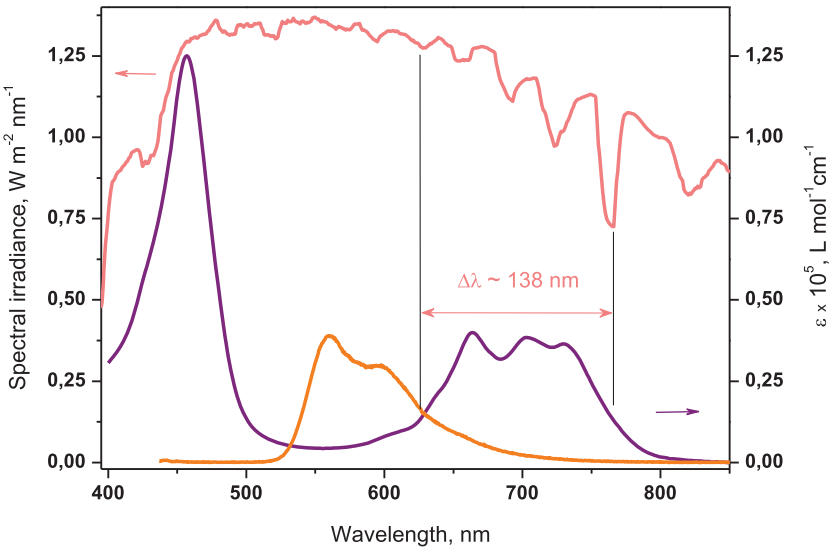

Fig. 10 Molar extinction of a sensitizer blend composed of mixed benzo-naphtho porphyrin family (**14**) and mixed naphtho-anthra porphyrin family (**27**) in molar ratio 1 : 2, total molar concentration 1×10^{-5} M (the violet line); Sun spectral irradiance (pink line), AM 1.5; fluorescence spectrum of the emitter—rubrene (orange line). For simplicity, the emitter fluorescence spectrum is normalized regarding the Q-band absorption of the sensitizer ensemble.

4 Conclusion

We report chemical synthesis of a sensitizer ensemble consisting of a mixed benzo-naphtho porphyrin family and mixed naphtho-anthra porphyrin family with an unprecedentedly broad Q-band absorption spectrum—as broad as $\Delta\lambda \sim 142$ nm (FWHM), optimized for the process of TTA photon energy upconversion. The corresponding UCd harvests in a gap-free manner the entire deep-red part of the terrestrial solar irradiation and transfers its photon energy in a visible light with a central wavelength of a 560 nm.

Appendix A: Precursor Synthesis

A1 Benzo-Building Block

2-Formylcyclohexanone sodium salt (2): 11.5 g (0.5 mol) of sodium lumps were dissolved in 150 mL of methanol. Cyclohexanone **1** (49.0 g; 0.5 mol) and methylformate (30 g; 0.5 mol) were added during 10 min. The reaction was stirred at room temperature overnight. 100 mL diethyl ether was added, and the precipitate was filtered and dried. The resulting 2-formylcyclohexanone sodium salt **2** was obtained as a white powder with 62% yield (45.88 g; 0.31 mol). The product was subjected to synthesis without further analysis.

Ethyl-(*E*)-((2-oxocyclohexylidene)methyl)glycinate (3): 2-Formyl-cyclohexanone-sodium salt **2** (40.0 g, 0.27 mol) was dissolved in ethanol (300 mL), glycin-ethyl-ester-hydrochloride (37.69 g, 0.27 mol) was added, and the reaction was stirred overnight at room temperature. The solvent was evaporated under reduced pressure resulting in 70% (39.88 g; 0.19 mol) of ethyl-((2-oxocyclohexylidene)methyl)glycinate **3** as a white solid. The product was subjected to synthesis without further analysis.

Ethyl-4,5,6,7-tetrahydro-2*H*-isoindole-1-carboxylate (4): Sodium lumps (2.3 g, 0.10 mol) were dissolved in 200 mL ethanol, 20 g (0.10 mol) ethyl-((2-oxocyclohexylidene)methyl)glycinate **3** was added, and the resulting solution was heated for 5 h at 40°C (Fig. 2). Afterward, the reaction mixture was allowed to cool down to room temperature. The product was extracted with DCM, which was further evaporated in vacuum. Recrystallization from a 1 : 1 mix of ethanol and DCM yielded 30% (5.79 g, 0.03 mol) white crystalline ethyl-4,5,6,7-tetrahydro-2*H*-isoindole-1-carboxylate 4. ^{1}H-NMR (300 MHz, CD_2Cl_2): δ (ppm) 8.87 (br, s, 1H), 6.65 (d, 1H), 4.26 (q, 2H), 2.84–2.74 (m, 2H), 2.59–2.50 (m, 2H), 1.77–1.69 (m, 4H), and 1.36–1.29 (t, 3H).

4,5,6,7-Tetrahydro-2*H*-isoindole (B): Ethyl-4,5,6,7-tetrahydro-2H-isoindole-1-carboxylate **4** (3.0 g, 0.02 mol) and three pieces of potassiumhydroxide were dissolved in 30 mL of ethylenglykol and refluxed for 60 min under nitrogen atmosphere. After cooling down to room temperature, the reaction mixture was poured into water, the organic layer separated, washed with water, dried over sodiumsulfate, and concentrated through distillation in vacuum. Flash chromatography yielded 4,5,6,7-tetrahydro-2*H*-isoindole **B** (1.26 g, 0.01 mol, 67%).

A2 Naphtho-Building Block

1,4-Dihydronaphthalene (6): 50.00 g (0.39 mol) naphthalene **5** was dissolved in 500-mL ethanol. 50.00 g (2.00 mol) sodium was added within 20 min. Water was added, and the solution was extracted with DCM. After the solvent was evaporated under reduced pressure, 40.61 g (0.31 mol, 80% yield) of liquid 1,4-dihydronaphthalene **6** was obtained. The product was subjected to synthesis without further analysis.

(3-Chloro-1,2,3,4-tetrahydronaphthalen-2-yl)(phenyl)sulfane (7): NCS (41.1 g, 0.31 mol) was dissolved in 200 mL DCM in a flask with argon atmosphere. After complete addition of 33.91 g (0.31 mol) thiophenol, the mixture was stirred for an additional 30 min. Subsequently, 1,4-dihydronaphthalene **6** (40.60 g, 0.31 mol) was mixed with 200-mL DCM in a flask with argon atmosphere. Phenylsulfenylchloride was added slowly, and the resulting mixture was stirred for an additional 30 min. The solvent was evaporated under reduced pressure, leaving 76.95 g (0.28 mol, 90% yield) (3-chloro-1,2,3,4-tetrahydronaphthalen-2-yl)(phenyl)sulfane **7**.

2-Chloro-3-(phenylsulfonyl)-1,2,3,4-tetrahydronaphthalene (8): (76.95 g, 0.28 mol) of (3-chloro-1,2,3,4-tetrahydronaphthalen-2-yl)(phenyl)sulfane **7** was dissolved in 200 mL THF and cooled with an ice bath. Oxone (85.23 g, 0.56 mol) dissolved in 200-mL water was added. The mixture was allowed to stir at room temperature for 2 days. Thereafter, it was diluted with 500 mL water and extracted with DCM. The solvent was evaporated, and the crude product was recrystallized from ethanol. This resulted in 49.02 g (0.16 mol, 57% yield) of yellowish 2-chloro-3-(phenylsulfonyl)-1,2,3,4-tetrahydronaphthalene **8**.

2-(Phenylsulfonyl)-1,2-dihydronaphthalene (9): 2-chloro-3-(phenylsulfonyl)-1,2,3,4-tetrahy-dro-naphthalene **8** (49.02 g, 0.16 mol) was dissolved in DCM, and DBU (25.10 g, 0.16 mol) was added. The reaction mixture was stirred for 30 min. The mixture was washed with water and dried, and the solvent was evaporated under reduced pressure. Recrystallization from ethanol yielded 24.31 g (0.09 mol, 56%) 2-(phenylsulfonyl)-1,2-dihydro-naphthalene **9**.

t-Butyl 4,9-dihydro-2*H*-benzo[*f*]isoindole-1-carboxylate (10): In a flask with potassium tert-butoxide (4.49 g, 0.04 mol) dissolved in 20-mL THF, t-butyl-cyanoacetate (5.65 g, 0.04 mol) was added. 2-(Phenylsulfonyl)-1,2-dihydro-naphthalene **9** (11.19 g, 0.04 mol) was added under argon atmosphere and stirred for 2 h. The solvent was evaporated, the crude product was washed with water and extracted with DCM. After evaporation to dryness, recrystallization from ethanol resulted in the t-butyl ester protected 4,9-dihydro-2*H*-benzo[*f*]isoindole **10** with 43% yield (4.85 g, 0.02 mol). ^{1}H-NMR (300 MHz, CD_2Cl_2): δ (ppm) 9.12 (br, 1H), 7.33–7.23 (d, 2H), 7.20–7.14 (d, 2H), 6.80 (s, 1H), 4.15–4.10 (d, 2H), 3.92–3.86 (d, 2H), 1.61 (s, 3H).

4,9-Dihydro-2*H*-benzo[*f*]isoindole (N): t-Butyl 4,9-dihydro-2*H*-benzo[f]isoindole-1-carboxylate **10** (4.83 g, 0.02 mol) and three pieces of potassiumhydroxide were dissolved in 30 mL of ethylenglykol and refluxed for 60 min under nitrogen atmosphere. After cooling down to room temperature, the reaction mixture was poured into water, the organic layer separated, washed with water, dried over sodiumsulfate, and concentrated through distillation in vacuum. Flash chromatography yielded 4,9-dihydro-2*H*-benzo[*f*]isoindole **N** (1.26 g, 0.01 mol, 67%).

A3 Anthra-Building Block

1,4-Dihydro-1,4-epoxynaphthalene (17). 1,2-Dibromobenzene **15** (60.00 g, 0.25 mol) and furan **16** (17.00 g, 0.25 mol) were dissolved in 500-mL THF. The reaction mixture was cooled to −50°C under argon atmosphere. n-Buli (16.00 g, 0.25 mol) in hexane was added slowly. The mixture was stirred for an additional 30 min at −50°C. Subsequently, 10 mL water was added, and, after the mixture reached room temperature, the solvent was evaporated under

reduced pressure. This resulted in 31.12 g (0.22 mol, 86% yield) of 1,4-dihydro-1,4-epoxynaphthalene **17**.

1,4,4a,9,9a,10-Hexahydro-9-10-epoxyanthracene (18): 1,4-dihydro-1,4-epoxynaphthalene **17** (30.96 g, 0.22 mol) and 3-sulfolene (25.37 g, 0.22 mol), $NaHCO_3$ (0.76 g, 0.009 mol), and 15 mL pyridine were added to a high-pressure glass flask and heated 18 h at 120°C. Upon completion, the mixture was filtered and the solvent evaporated under reduce pressure. Flash chromatography with DCM as the eluent resulted in a beige powder of 1,4,4a,9,9a,10-hexahydro-9-10-epoxyanthracene **18** with 48% yield (20.31 g, 0.10 mol).

1,4-Dihydroanthracene (19): 1,4,4a,9,9a,10-hexahydro-9-10-epoxyanthracene **18** (20.31 g, 0.10 mol) was dissolved in 400-mL ethanol in a flask under argon atmosphere. 20-mL concentrated hydrochloric acid was added and the reaction mixture was refluxed overnight. The solvent was evaporated under reduced pressure and the crude product was recrystallized from ethanol, resulting in 56% (10.44 g, 0.06 mol) of 1,4-dihydroanthracene **19**.

(3-Chloro-1,2,3,4-tetrahydroanthracene-2-yl)(phenyl)sulfane (20): NCS (7.41 g, 0.06 mol) was dissolved in 50-mL DCM in a flask with argon atmosphere. After complete addition of 6.11 g (0.06 mol) thiophenol, the mixture was stirred for an additional 30 min. Subsequently, 1,4-dihydroanthracene **19** (10.20 g, 0.06 mol) was mixed with 50-mL DCM in a flask with argon atmosphere. Phenylsulfenylchloride **7** was added slowly and the resulting mixture stirred for an additional 30 min. The solvent was evaporated under reduced pressure, leaving 17.81 g (0.05 mol, 91% yield) (3-chloro-1,2,3,4-tetrahydroanthracene-2-yl)(phenyl)sulfane **20**.

2-Chloro-3-(phenylsulfonyl)-1,2,3,4-tetrahydroanthracene (21): 17.72 g (0.05 mol) of 3-chloro-1,2,3,4-tetrahydroanthracene-2-yl)(phenyl)sulfane **20** was dissolved in 50-mL THF and cooled with an ice bath. Oxone (16.74 g, 0.11 mol), dissolved in 30-mL water, was added. The mixture was allowed to stir at room temperature for 2 days. Thereafter, it was diluted with 30 mL water and extracted with DCM. The solvent was evaporated and the crude product was recrystallized from ethanol. This resulted in 10.71 g (0.03 mol, 55% yield) of yellowish 2-chloro-3-(phenylsulfonyl)-1,2,3,4-tetrahydroanthracene **21**.

2-(Phenylsulfonyl)-1,2-dihydroanthracene (22): 2-chloro-3-(phenylsulfonyl)-1,2,3,4-tetrahy-droanthracene **21** (10.65 g, 0.03 mol) was dissolved in DCM and DBU (4.57 g, 0.03 mol) was added. The reaction mixture was stirred for 30 min. The mixture was washed with water and dried, and the solvent was evaporated under reduced pressure. Recrystallization from ethanol yielded 6.41 g (0.02 mol, 72%) 2-(phenylsulfonyl)-1,2-dihydro-anthracene **22**.

Ethyl 4,11-dihydro-2*H*-naphtho[2,3-*f*]isoindole-1-carboxylate (23): In a flask with potassium tert-butoxide (1.27 g, 0.01 mol) was dissolved in 20 mL THF, and ethyl-2-cyanoacetate (1.28 g, 0.01 mol) was added. 2-(Phenylsulfonyl)-1,2-dihydroanthracene **22** (3.63 g, 0.01 mol) was added under argon atmosphere and stirred for 2 h. The solvent was evaporated; the crude product was washed with water and extracted with DCM. After evaporation to dryness, recrystallization from ethanol resulted in ethyl 4,11-dihydro-2*H*-naphtho[2,3-*f*]isoindole-1-carboxylate **23** with 53% yield (1.75 g, 0.006 mol). The obtained ^{1}H-NMR (250 MHz, d-toluol) displayed peaks with following chemical shifts: δ (ppm) 8.22 (br, 1H), 7.66–7.56 (m, 2H), 7.54–7.45 (d, 2H), 7.29–7.23 (d, 2H), 6.16 (s, 2H), 4.37 (s, 2H), 4.15–4.13 (dd, 2H), 3.79 (s, 2H), and 1.20–1.10 (t, 3H).

4,11-Dihydro-2*H*-naphtho[2,3-*f*]isoindole (A): Ethyl 4,11-dihydro-2*H*-naphtho[2,3-*f*]isoindole-1-carboxylate **23** (1.39 g, 0.005 mol) and three pieces of potassiumhydroxide were dissolved in 30 mL of ethylenglykol and refluxed for 60 min under nitrogen atmosphere. After cooling down to room temperature, the reaction mixture was poured into water; the organic layer was separated, washed with water, dried over sodiumsulfate, and concentrated through distillation in vacuum. Flash chromatography yielded 4,11-dihydro-2*H*-naphtho[2,3-*f*]isoindole **A** (669 mg, mol, 61%).

Acknowledgments

This work was performed under the European Union's Horizon 2020 Research and Innovation Program under Grant agreement No. 732794—project HYPOSENS. S. Baluschev acknowledges also the DFNI E 02/11—SunStore-project of the Bulgarian National Science Fund. The authors declare no competing financial interests or other potential conflict of interests.

References

1. A. Luque and A. Marti, "Increasing the efficiency of ideal solar cells by photon induced transitions at intermediate levels," *Phys. Rev. Lett.* **78**, 5014–5017 (1997).
2. A. Nattestad et al., "Highly efficient photocathodes for dye-sensitized tandem solar cells," *Nat. Mater.* **9**(1), 31–35 (2010).
3. R. Islangulov et al., "Noncoherent low-power upconversion in solid polymer films," *J. Am. Chem. Soc.* **129**(42), 12652–12653 (2007).
4. S. Baluschev et al., "Blue-green up-conversion: non-coherent excitation by NIR-light," *Angew. Chem. Int. Ed.* **46**(40), 7693–7696 (2007).
5. A. Lebedev et al., "Dendritic phosphorescent probes for oxygen imaging in biological systems," *ACS Appl. Mater. Interfaces* **1**, 1292–1304 (2009).
6. T. N. Singh-Rachford et al., "Boron dipyrromethene chromophores: next generation triplet acceptors/annihilators for low power upconversion schemes," *J. Am. Chem. Soc.* **130**, 16164–16165 (2008).
7. R. E. Keivanidis et al., "Inherent photon energy recycling effects in the up-converted delayed luminescence dynamics of poly(fluorene)-Pt(II)octaethyl porphyrin blends," *ChemPhysChem* **10**(13), 2316–2326 (2009).
8. Y. Cheng et al., "Kinetic analysis of photochemical upconversion by triplet–triplet annihilation: beyond any spin statistical limit," *Phys. Chem. Lett.* **1**(12), 1795–1799 (2010).
9. A. Monguzzi et al., "Efficient broadband triplet–triplet annihilation-assisted photon upconversion at subsolar irradiance in fully organic systems," *Adv. Funct. Mater.* **25**, 5617–5624 (2015).
10. K. Borjesson et al., "Photon upconversion facilitated molecular solar energy storage," *J. Mater. Chem. A* **1**, 8521–8524 (2013).
11. Y. C. Simon et al., "Low-power upconversion in dye-doped polymer nanoparticles," *Macromol. Rapid Commun.* **33**, 498 (2012).
12. S. H. C. Askes et al., "Imaging the lipid bilayer of giant unilamellar vesicles using red-to-blue light upconversion," *Chem. Commun.* **51**, 9137 (2015).
13. M. Filatov et al., "Tetraaryltetraanthra[2, 3]porphyrins: synthesis, structure and optical properties," *J. Org. Chem.* **77**, 11119–11131 (2012).
14. M. Filatov et al., "SPIE Newsroom," 7 April 2014, http://spie.org/x106642.xml.
15. M. I. J. Lorenz, S. H. Fischer, and O. S. Wolfbeis, "Multiple fluorescent chemical sensing and imaging," *Chem. Soc. Rev.* **39**, 3102–3114 (2010).
16. M. A. Filatov, S. Baluschev, and K. Landfester, "Protection of densely populated excited triplet state ensembles against deactivation by molecular oxygen," *Chem. Soc. Rev.* **45**, 4668–4689 (2016).
17. S. Baluschev et al., "Annihilation upconversion in nanoconfinement: solving the oxygen quenching problem," *Mater. Horiz.* **3**, 478–486 (2016).
18. Q. Liu et al., "A general strategy for biocompatible, high-effective upconversion nanocapsules based on triplet–triplet annihilation," *J. Am. Chem. Soc.* **135**, 5029–5037 (2013).
19. O. Finikova et al., "An expedient synthesis of substituted tetraaryltetrabenzoporphyrins," *Chem. Commun.* **3**, 261–262 (2001).
20. M. Brunel et al., "Reverse saturable absorption in palladium and zinc tetraphenyltetrabenzoporphyrin doped xerogels," *Chem. Phys.* **218**, 301–307 (1997).
21. M. A. Filatov et al., "Reversible oxygen addition on a triplet sensitizer molecule: protection from excited state depopulation," *Phys. Chem. Chem. Phys.* **17**, 6501–6510 (2015).
22. M. A. Filatov et al., "Meso-tetraphenylporphyrin with a pi-system extended by fusion with anthraquinone," *Org. Biomol. Chem.* **13**, 6977–6983 (2015).
23. R. Leutz and A. Suzuki, *Nonimaging, Fresnel Lenses: Design and Performance of Solar Concentrators*, Springer-Verlag, Berlin, Heidelberg (2001).
24. J. Mendes-Lopes et al., "New Fresnel Köhler optical design: 9-fold photovoltaic concentrator," *Proc. SPIE* **8834**, 88340A (2013).
25. S. Karabasheva et al., "Microstructures on soluble polymer surfaces via drop deposition of solvent mixtures," *Appl. Phys. Lett.* **89**(3), 031110 (2006).

26. J. Y. Kim et al., "Hybrid polymer microlens arrays with high numerical apertures fabricated using simple ink-jet printing technique," *Opt. Mater. Express* **1**(2), 259–269 (2011).
27. M. Hu et al., "A microlens array based on polymer network liquid crystal," *J. Appl. Phys.* **113**(5), 053105 (2013).
28. X. Zhang et al., "Control of polymer phase separation by roughness transfer printing for 2D microlens arrays," *Small* **12**(28), 3788–3793 (2016).

Ernesta Heinrich received her diploma from the University of Mainz, Germany, in 2016. Currently, she is pursuing her PhD at Max Planck Institute for Polymer Research in Mainz, Germany. Her research focuses on the synthesis of organic dyes, specifically sensitizers molecules for TTA-UC.

Yuri Avlasevich received his MS degree in organic chemistry from Belarusian State University in 1993 and his PhD in polymer chemistry from the Institute of Physical Organic Chemistry, National Academy of Sciences, Minsk, Belarus, in 2000. After being visiting scientist at the Institute of Physical Chemistry in Warsaw, Poland, and Institute of General Botany, University of Mainz, he joined in 2009 the Physical Chemistry of Polymers Group, where he is working now as research chemist in the field of upconverting dyes.

Katharina Landfester received her doctoral degree in physical chemistry after working with professor H. W. Spiess at the MPIP in 1995. She joined the Max Planck Society in 2008 as one of the directors of the MPI for Polymer Research. She studied chemistry at the Technical University of Darmstadt and in Strasbourg. In 1996, she moved for a doctoral stay at Lehigh University in 1998 at the MPI of colloids and interfaces in Golm. In 2003, she accepted a chair (C4) of macromolecular chemistry at the University of Ulm.

Stanislav Baluschev studied laser physics at Sofia University "Saint Kliment Ochridski," Bulgaria, where he received his PhD. In 1996, he was granted a DAAD Research fellowship at Hannover University, Germany; in 1999—a Feinberg Research Fellowship at the Department of Complex Systems, Weizmann Institute of Science, Israel; during the of the academic year 2014–2015, he was an FRIAS-senior fellow, University of Freiburg, Germany. In 2001, he joined the group of professor Gerhard Wegner/professor Katharina Landfester at MPI for Polymer Research. His current research interests include nonlinear optics, atomic physics, and annihilation upconversion.